High expression of Sam68 contributes to metastasis by regulating vimentin expression and a motile phenotype in oral squamous cell carcinoma

TAKUYA KOMIYAMA[1], TAKESHI KUROSHIMA[1], TAKEHITO SUGASAWA[2], SHIN-ICHIRO FUJITA[2], YUTA IKAMI[1], HIDEAKI HIRAI[1], FUMIHIKO TSUSHIMA[1], YASUYUKI MICHI[1], KOU KAYAMORI[3], FUMIHIRO HIGASHINO[4-6] and HIROYUKI HARADA[1]

[1]Department of Oral and Maxillofacial Surgical Oncology, Division of Health Science, Graduate School of Medical and Dental Sciences, Tokyo Medical and Dental University, Bunkyo-ku, Tokyo 113-8549; [2]Laboratory of Clinical Examination/Sports Medicine, Department of Clinical Medicine, Faculty of Medicine, University of Tsukuba, Tsukuba, Ibaraki 305-8577; [3]Department of Oral Pathology, Division of Oral Health Science, Graduate School of Medical and Dental Sciences, Tokyo Medical and Dental University, Bunkyo-ku, Tokyo 113-8549; [4]Department of Molecular Oncology, Faculty of Dental Medicine and Graduate School of Biomedical Science and Engineering; [5]Department of Vascular Biology and Molecular Pathology, Faculty of Dental Medicine and Graduate School of Dental Medicine, Hokkaido University, Sapporo, Hokkaido 060-8586, Japan

Received May 17, 2022; Accepted July 18, 2022

DOI: 10.3892/or.2022.8398

Abstract. The present study aimed to investigate the clinical and biological significance of Src-associated in mitosis 68 kDa (Sam68) in oral squamous cell carcinoma (OSCC). Immunohistochemical analysis was performed on tissue samples obtained from 77 patients with OSCC. Univariate analysis revealed that the high expression of Sam68 was significantly correlated with advanced pathological T stage (P=0.01), positive lymphovascular invasion (P=0.01), and pathological cervical lymph node metastasis (P<0.01). Moreover, multivariate analysis demonstrated that the high expression of Sam68 was an independent predictive factor for cervical lymph node metastasis (odds ratio, 4.39; 95% confidence interval, 1.49-14.23; P<0.01). These results indicated that high Sam68 expression contributed to tumor progression, especially cervical lymph node metastasis, in OSCC. mRNA sequencing was also performed to assess the changes in the transcriptome between OSCC cells with Sam68 knockdown and control cells with the aim of elucidating the biological roles of Sam68. Gene Ontology enrichment analysis revealed that downregulated differentially expressed genes (DEGs) were concentrated in some biological processes related to epithelial-mesenchymal transition. Among these DEGs, it was established that vimentin was particularly downregulated in these cells. It was also confirmed that Sam68 knockdown reduced the motility of OSCC cells. Furthermore, the immunohistochemical study of vimentin identified the association between vimentin expression and Sam68 expression as well as cervical lymph node metastasis. In conclusion, the present study suggested that the high expression of Sam68 may contribute to metastasis by regulating vimentin expression and a motile mesenchymal phenotype in OSCC.

Correspondence to: Dr Takeshi Kuroshima, Department of Oral and Maxillofacial Surgical Oncology, Division of Health Science, Graduate School of Medical and Dental Sciences, Tokyo Medical and Dental University, 1-5-45 Yushima, Bunkyo-ku, Tokyo 113-8549, Japan
E-mail: kuroosur@tmd.ac.jp

Present address: [6]Department of Medical Management and Informatics, Faculty of Medical Informatics, Hokkaido Information University, Ebetsu, Hokkaido 069-8585, Japan

Abbreviations: DEG, differentially expressed genes; DMEM, Dulbecco's modified Eagle's medium; EMT, epithelial-mesenchymal transition; FBS, fetal bovine serum; GO, Gene Ontology; OSCC, oral squamous cell carcinoma; PBS, phosphate-buffered saline; PCR, polymerase chain reaction; Sam68, Src-associated in mitosis 68 kDa; SCC, squamous cell carcinoma; YK, Yamamoto-Kohama

Key words: Src-associated in mitosis 68 kDa, vimentin, epithelial-mesenchymal transition, motility, metastasis, oral cancer

Introduction

Oral cancer is one of most common malignancies worldwide, with an estimated 354,864 new cases and 177,384 cancer-related deaths occurring in 2018 (1). The major pathology of oral cancer is squamous cell carcinoma (SCC) (2). Despite advances in the diagnosis and treatment of oral squamous cell carcinoma (OSCC), the prognosis of patients with advanced OSCC has not been improved in the past four decades (3). Metastasis to

the cervical lymph nodes is an accurate prognostic factor for patients with OSCC (4-7); however, its molecular mechanism remains unclear. Therefore, there is a need for studies investigating crucial biomarkers and therapeutic targets of metastasis in OSCC.

Src-associated in mitosis 68 kDa (Sam68) was originally identified as the first mitotic substrate of the tyrosine kinase Src and belongs to the signal transduction and activation of RNA family of RNA-binding proteins (8,9). These proteins contain a GRP33/SAM68/GLD-1 domain formed by a single heterogenous nuclear ribonucleoprotein particle K homology domain and two flanking regions for RNA-binding (8-10). Although Sam68 is predominantly localized in the nucleus, it can shuttle between the nucleus and the cytoplasm, depending on its functions (9-12). Sam68 has been implicated in RNA metabolism, including transcription, alternative splicing, transport, and translation (12-15). Sam68 is involved in multiple biological events, including cell-cycle regulation, apoptosis, response to conditions of external stress, bone metabolism, neural functions, and viral infection (10,12,13,16,17).

A series of previous studies has also shown a pro-oncogenic role of Sam68 via the regulation of the signal transduction pathway, transcription of cancer-related genes, alternative splicing events, and noncoding RNAs (13,14,18,19). Researchers have reported that in different types of human cancers, the dysregulation of Sam68 is implicated in tumorigenesis, tumor progression, and patient prognosis (20-26). Nonetheless, it remains unclear whether Sam68 has clinical and biological significance in OSCC.

Therefore, the aim of the present study was to investigate the correlation between Sam68 expression and clinicopathological features in OSCC via immunohistochemical analysis and to elucidate the biological roles of Sam68 in OSCC cells.

Materials and methods

Patients and tissue specimens. A total of 77 patients diagnosed with pathologically confirmed SCC of the tongue, who underwent radical surgery at the Department of Oral Maxillofacial Surgery at Tokyo Medical and Dental University Hospital (Tokyo, Japan), between 2014 and 2017, were enrolled in this retrospective study. Patients who had previously received any treatment for tongue cancer were excluded from the study. The surgical specimens were obtained from formalin-fixed paraffin-embedded tissues. Clinical data on patient age, sex, TNM classification, pathological differentiation of the primary tumor, the mode of invasion according to Yamamoto-Kohama (YK) classification (27), perineural invasion, lymphovascular invasion, surgical margins, pathological cervical lymph node metastases, and treatment outcomes were obtained from the medical records of patients. No patients received radiotherapy or chemotherapy before radical surgery. Clinical staging was based on the TNM staging system of the American Joint Committee on Cancer, seventh edition (28).

This study complied with the Declaration of Helsinki and was approved (approval no. D2020-025) by the Institutional Review Board of Tokyo Medical and Dental University. Opt-out informed consent from patients was obtained by exhibiting the research information on the official website of the hospital (Tokyo Medical and Dental University Hospital, Tokyo, Japan). The authors guarantee the opportunity for refusal by document, call or e-mail whenever possible. Patients who rejected participation in this study were excluded.

Immunohistochemistry. The surgical specimens were fixed with 10% formalin for 24 h at room temperature and then embedded with paraffin. The paraffin-embedded tissue blocks of the specimens were cut into 4-μm serial sections and examined immunohistochemically. The sections were deparaffinized with xylene and rehydrated through a series of graded alcohol concentrations, followed by transfer and rinse with phosphate-buffered saline (PBS). The epitopes were then retrieved by autoclave in 0.01 M citrate buffer at 121˚C for 15 min. After cooling, endogenous peroxidase activity was blocked by 3% hydrogen peroxide in methanol at room temperature for 15 min and treated with 10% goat serum (Nichirei Biosciences, Inc.) at room temperature for 15 min to prevent nonspecific binding. The slides were washed three times with PBS and incubated overnight at 4˚C with monoclonal rabbit anti-SAM68 (dilution 1:100; cat. no. ab76471; Abcam) or polyclonal rabbit anti-vimentin (dilution 1:3,000, cat. no. 10366-1-AP; ProteinTech Group, Inc.). Following additional washing with PBS three times, the sections were incubated with a biotin-conjugated anti rabbit secondary antibody, which was included in a Histofine SAB-PO(R) kit (cat. no. 424031; Nichirei Biosciences, Inc.) and used in undiluted form, at room temperature for 10 min. Reactive products were detected using this kit, followed by visualization using the Histofine DAB-3S kit (Nichirei Biosciences, Inc.) and counterstain with hematoxylin.

Two independent observers who were blinded to the clinical data analyzed the sections. Doubtful cases were reassessed, and discrepancies were settled by consensus. The expression of Sam68 was determined in the nucleus and cytoplasm by semiquantitative assessment of the percentage of positively stained tumor cells and staining intensity under a light microscope in three representative fields on each slide (Olympus System Microscope Model BX43; Olympus Corporation). The percentage of positive cells was scored as follows: 1 (0-50% positive cells) and 2 (51-100% positive cells). Staining intensity was scored as follows: 0, no signal; 1, weak; 2, moderate; and 3, strong. The staining index was calculated as the production of the score for the percentage of positive cells and staining intensity. The nuclear and cytoplasmic indices were calculated (scores of 0, 1, 2, 3, 4, and 6, respectively). The total index was determined as Sam68 expression by summing the nuclear and cytoplasmic indices (scores of 0-12). The validity of the optimal cutoff value for each categorical variable was determined using receiver-operating characteristic curve analysis. A total index ≥8 was considered high expression in the OSCC tissues. Staining for vimentin was classified as negative and positive if cytoplasmic immunostaining occurred in <10% and ≥10% of epithelial tumor cells, respectively (29,30).

Cell lines. HO-1-N-1 (a human buccal mucosal SCC cell line), HSC-2 (a human oral SCC cell line), HSC-3 (a human tongue SCC cell line), and HOC-313 (a human floor-of-the mouth SCC cell line) were cultured at 37˚C in a 5% CO_2 atmosphere in Dulbecco's modified Eagle's medium (DMEM) (Nacalai

Tesque, Inc.) containing 10% fetal bovine serum (FBS; Nichirei Biosciences, Inc.). HO-1-N-1 was purchased from the Japanese Collection of Research Bioresources (cat. no. JCRB0831). HSC-2, HSC-3, and HOC-313 were established from surgical resected tumors at the Department of Oral and Maxillofacial Surgery, Tokyo Medical and Dental University (31,32).

Western blot analysis. Whole-cell lysates were prepared using radioimmunoprecipitation lysis buffer (Santa Cruz Biotechnology, Inc.) containing protease inhibitors. Protein content of the samples was measured using a Qubit Fluorimeter and Qubit Protein Assay Kits (Thermo Fisher Scientific, Inc.). Next, 20 μg of each sample was separated by 10% sodium dodecyl sulfate-polyacrylamide gel electrophoresis and transferred onto nitrocellulose membranes (BioRad Laboratories, Inc.). Membranes were blocked with 5% non-fat milk (TPBT) at room temperature for 60 min, then incubated with monoclonal rabbit anti-SAM68 (dilution 1:500; cat. no. ab76471; Abcam) or β-actin (1:4,000; cat. no. ab76471; ProteinTech Group, Inc.) at room temperature for 60 min. The total protein content was confirmed by β-actin staining. After washing with PBS, membranes were incubated with a horseradish peroxidase (HRP)-conjugated anti rabbit secondary antibody dilution 1:4,000; cat. no. 7074; Cell Signaling Technology) at room temperature for 60 min. Immunoreactive bands were visualized with chemiluminescence using Pierce ECL Western Blotting Substrate or SuperSignal West Dura Extended Duration Substrate (both from Thermo Fisher Scientific, Inc.).

Sam68 knockdown. Sam68 small interfering RNA (siRNA)#1 (5'-GCAAAGUUGUUACUGAUUU-3'; MISSION predesigned siRNA), Sam68 siRNA#2 (5'-GAGCAAAGUUGUUACUGAU-3'; MISSION predesigned siRNA; both from Sigma-Aldrich: Merck KGaA), and control siRNA (Silencer Negative Control No. 1 siRNA; cat. no. AM4611; Ambion; Thermo Fisher Scientific, Inc.) were transfected into cells (60-70% confluence) using HilyMax (Dojindo Laboratories, Inc.) transfection reagent at 37˚C according to the manufacturer's instructions. The concentration of each siRNA was 210 nM. The medium was replaced with fresh serum-containing medium at 4 h after the transfection. To evaluate the efficacy of gene silencing, Sam68 protein was assessed by western blotting at 48 and 144 h after the transfection.

RNA extraction and quantitative real-time reverse transcription polymerase chain reaction (RT-qPCR). Total cellular RNA was isolated using the RNeasy Mini Kit (Qiagen GmbH), according to the manufacturer's protocol. Total RNA (2 μg) was reverse-transcribed using ReverTra Ace qPCR RT Master Mix (TOYOBO, Inc.). The ABI 7500 real-time polymerase chain reaction (PCR) system and SYBR Green Real-time PCR Master Mix Plus (TOYOBO, Inc.) were used for quantitative reverse transcription PCR (RT-qPCR). The PCR amplification profile was as follows: Initial denaturation at 95˚C for 5 min, followed by 40 cycles of denaturation at 95˚C for 15 sec and annealing and extension at 60˚C for 60 sec. All expression data were normalized to the expression of β-actin. The primers used in this assay are listed in Table SI. The $2^{-\Delta\Delta Cq}$ method was used for relative quantification of gene expression levels (33).

mRNA sequencing, differential expression analysis, and gene ontology (GO) enrichment analysis. At 48 h after transfection, total cellular RNA was obtained from the sample of HO-1-N-1 cells with Sam68 siRNA#1 or control siRNA using the RNeasy Mini Kit (Qiagen GmbH) according to the manufacturer's instructions. Samples were prepared for each group to perform three independent assays. mRNA sequencing was performed using Illumina NextSeq500 (Illumina, Inc.) at the Department of Sports Medicine Analysis under the Open Facility Network Office, University of Tsukuba, in accordance with the standard protocol (34). Sequencing was conducted with paired-end reads of 36 bases. After the sequencing run, the FASTQ files were exported and the basic information of the NGS run data was verified using CLC Genomics Workbench 20.0.3 software (Qiagen GmbH). Quality assessment of the reads confirmed a PHRED score (quality value) of >20 for 99.68% of all reads, indicating the success of the run. The read number was approximately 35.4-37.5 million per sample as paired-end reads. The RNA sequencing data as FASTQ files and expression browser as table data are deposited in the Gene Expression Omnibus (https://www.ncbi.nlm.nih.gov/geo/) under accession number GSE202136. The Metascape tool (https://metascape.org/gp/index.htmls/main/step1) was used to perform GO enrichment analysis of differentially expressed genes (35).

Wound healing assay. After 48 h of Sam68 siRNA or control siRNA transfection, $1.0x10^6$ HO-1-N-1 cells were cultured in 24-well plates until confluent. A wound was made through the confluent monolayer with a 200-μl pipette tip. There were confluent cells on either side of the wound. The wells were rinsed with PBS to remove detached cells. The remaining cells were incubated with DMEM containing 0.5% FBS. At 72 h after wound creation, the wound areas were evaluated using a phase-contrast microscope (Olympus System Microscope Model CKX53; Olympus Corporation). All experiments were performed in triplicate.

Chamber migration assay. At 48 h after Sam68 siRNA or control siRNA transfection, HO-1-N-1 cells were detached with TrypLE express (Thermo Fisher Scientific, Inc.) and resuspended in serum-free DMEM. A total of $5x10^5$ cells were seeded into the upper chamber of a Falcon Cell Culture Insert with an 8-μm pore filter (Corning, Inc.). DMEM with 10% FBS was added to the lower chamber. Cells were allowed to migrate for 48 h. The filters were then fixed with 100% ice-cold methanol at room temperature for 15 min and stained with Carrazzi's hematoxylin (Muto Pure Chemicals Co., Ltd.) at room temperature for 15 min, followed by removal of nonmigrated cells with a cotton swab. The filters were mounted on glass slides, and migrated cells adhering to the bottom side of the chamber were counted using a light microscope at a magnification of x40. All experiments were performed in triplicate.

Statistical analyses. Mann-Whitney U test was used for continuous variables between the two groups. The associations between Sam68 expression and categorical variables of clinicopathological features were assessed using Fisher's exact

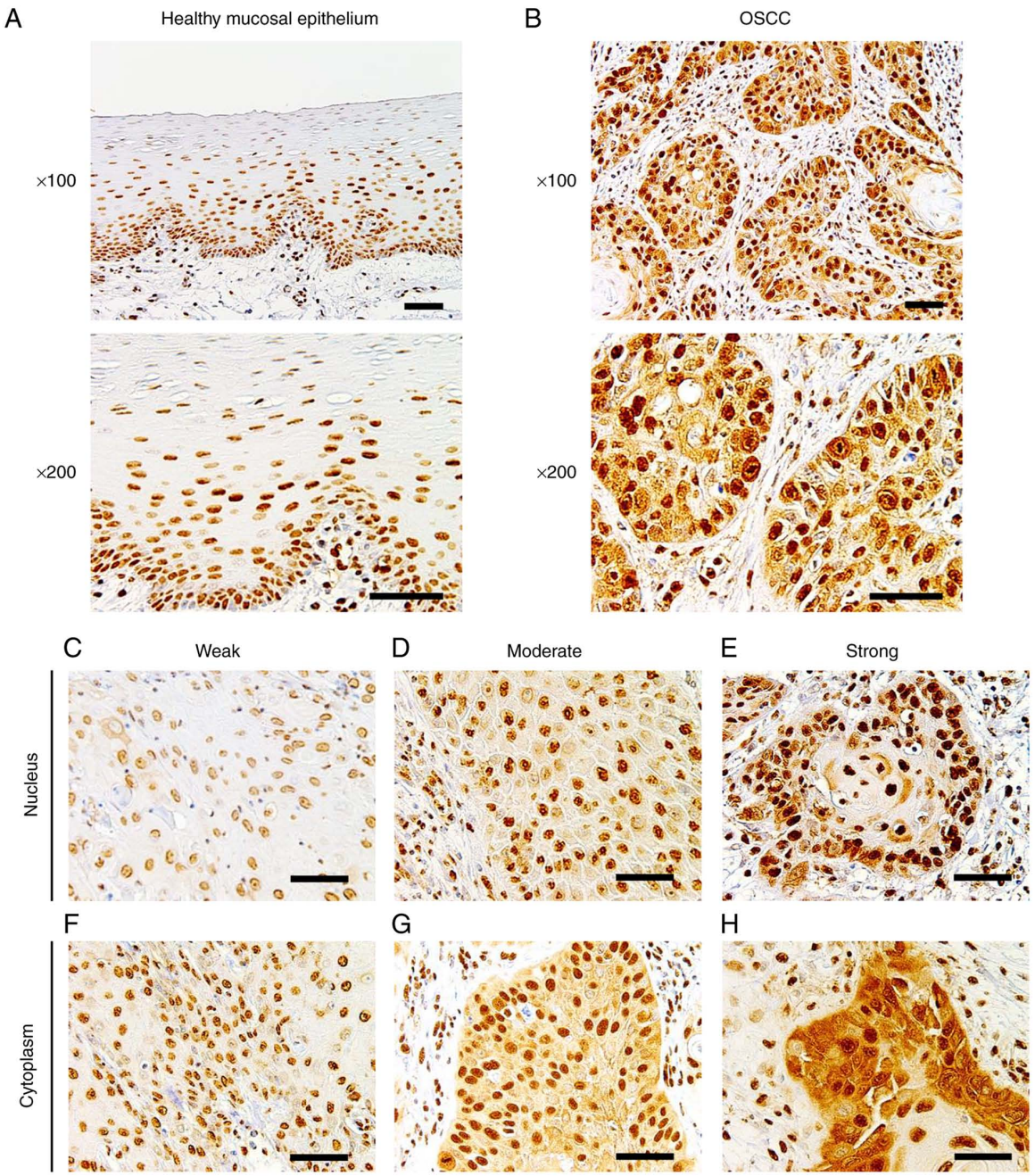

Figure 1. Immunohistochemistry of Sam68. (A) Representative images of healthy mucosal epithelium adjacent to OSCC, in which Sam68 expression was predominantly detected in the nucleus and negatively observed in the cytoplasm (magnification, x100 and x200; scale bar, 50 μm). (B) Representative image of OSCC, in which Sam68 expression was detected both in the nucleus and cytoplasm (magnification, x100 and x200; scale bar, 50 μm). (C-E) Nuclear expression of Sam68 with (C) weak, (D) moderate, and (E) strong staining intensity in OSCC cells (magnification, x200; scale bar, 50 μm). (F-H) Cytoplasmic expression of Sam68 with (C) weak, (D) moderate, and (E) strong staining intensity in OSCC tissue (magnification, x200; scale bar, 50 μm). Sam68, Src-associated in mitosis 68 kDa; OSCC, oral squamous cell carcinoma.

test or Pearson's chi-square test. To examine the correlation between Sam68 expression and clinicopathological features, multivariate logistic regression analysis was used. The results are expressed as the mean ± standard deviation (SD) in the wound healing assay, chamber migration assay, and RT-qPCR analysis. Statistical analyses of multiple comparisons were performed using one-way analysis of variance (ANOVA) with a post hoc Dunnett's test of all samples to control. $P<0.05$ was considered to indicate a statistically significant difference. All statistical analyses were performed using JMP14 (SAS Institute, Inc.).

Results

Sam68 expression in OSCC and adjacent healthy mucosa. To determine the expression of Sam68 in OSCC and healthy oral mucosa, immunohistochemical analysis was performed using the tissue samples of OSCC. In adjacent healthy mucosal epithelium, Sam68 expression was detected predominantly in the nucleus with moderate (52%) to strong (35%) intensity, whereas cytoplasmic Sam68 expression was mostly negative (72%), occasionally observed with weak intensity (23%), or rarely observed with moderate intensity (5%) (Fig. 1A). No case was confirmed

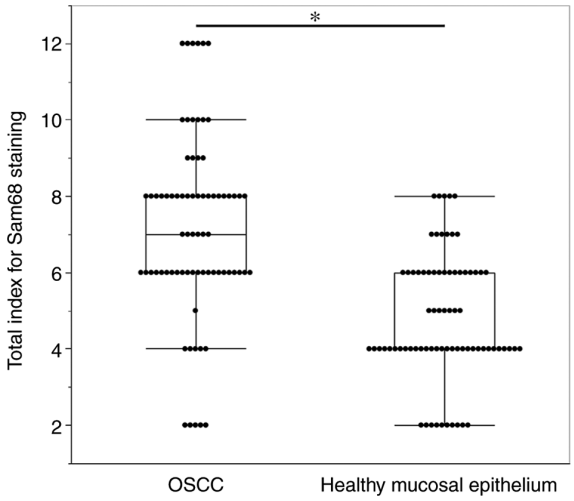

Figure 2. Comparison of the total staining index of Sam68 between OSCC cells and adjacent healthy mucosal epithelium. Mann-Whitney U test. *P<0.01. Sam68, Src-associated in mitosis 68 kDa; OSCC, oral squamous cell carcinoma.

to have cytoplasmic Sam68 expression with strong intensity in the adjacent healthy mucosal epithelium. By contrast, nuclear Sam68 expression with strong intensity was commonly observed (75%) in OSCC cells. Cytoplasmic Sam68 expression with moderate (25%) or strong intensity (16%) was observed in OSCC cells (Fig. 1B-H). As revealed in Fig. 2, the total staining index was significantly higher in OSCC (median index 7, interquartile range 6-8) than that of adjacent healthy mucosal epithelium (median index 4, interquartile range 4-6; P<0.01). These findings indicated that the expression of Sam68 was increased in OSCC compared with that of adjacent healthy epithelial cells.

Correlation between Sam68 expression and clinicopathological features in patients with OSCC. To investigate the clinical significance of Sam68 expression, the association between the total staining index of Sam68 and the clinicopathological features of patients with OSCC was analyzed. The results of the univariate analysis indicated that a high expression of Sam68 was significantly correlated with advanced pathological T stage (P=0.01), positive lymphovascular invasion (P=0.01), and pathological cervical lymph node metastasis (P<0.01; Table I).

Cervical lymph node metastasis is the most important prognostic factor in patients with OSCC; thus, additional statistical analyses were performed to assess whether Sam68 expression was a critical factor in pathological cervical lymph node metastasis. A significant correlation between pathological cervical lymph node metastasis and positive lymphovascular invasion (P=0.01) and the high expression of Sam68 (P<0.01; Table II) was observed. Moreover, multivariate logistic regression analysis revealed that a high expression of Sam68 was an independent factor for cervical lymph node metastasis [odds ratio (OR): 4.39; 95% confidence interval (CI): 1.49-14.23; P<0.01; Table III]. These results indicated that a high expression of Sam68 contributed to tumor progression, particularly cervical lymph node metastasis, in OSCC.

Sam68 expression and its knockdown in OSCC cells. For further investigation, the expression of Sam68 protein in OSCC cells was examined by western blotting. The expression

Table I. Univariate analyses of the correlation between Sam68 expression and clinicopathological features in patients with OSCC.

	Sam68 expression		
Clinicopathological features	Low (n=39)	High (n=38)	P-value
Age, years			0.56
<65	25	16	
>65	14	22	
Sex			0.05
Male	29	26	
Female	10	12	
pT			0.01[a]
T1 + T2	38	30	
T3 + T4	1	8	
Pathological differentiation			0.51
Well	20	15	
Moderate	16	18	
Poor	3	5	
YK classification			0.43
YK1 + YK2 + YK3	26	22	
YK4C + YK4D	13	16	
Lymphovascular invasion			<0.01
Negative	25	13	
Positive	14	25	
Perineural invasion			0.19[a]
Negative	36	31	
Positive	3	7	
Pathological CLNM			<0.01
Negative	33	19	
Positive	6	19	
Primary recurrence			0.99[a]
Negative	37	36	
Positive	2	2	

Pearson's chi-square test. [a]Fisher's exact test. P<0.05 was considered statistically significant in all analyses. OSCC, oral squamous cell carcinoma; CLNM, cervical lymph node metastasis; YK, Yamamoto-Kohama.

of Sam68 was detected in all OSCC cell lines (Fig. 3A). To examine the effect of Sam68, Sam68 knockdown in HO-1-N-1 cells was produced. From 48 to 144 h after the transfection, the expression of Sam68 was significantly decreased in Sam68 siRNA-transfected cells compared with that in control siRNA-transfected cells (Fig. 3B). These cells were subsequently used for the following experiments to assess the biological roles of Sam68 in OSCC.

Sam68 knockdown affects the phenotype of OSCC cells. To elucidate the potential mechanism by which Sam68 affects the phenotypes associated with metastasis in OSCC, mRNA

Table II. Univariate analysis of the correlation between clinicopathological features and lymph node metastasis.

Clinicopathological features	Pathological CLNM		P-value
	Negative (n=52)	Positive (n=25)	
Age, years			0.11
<65	27	14	
>65	25	11	
Sex			0.54
Male	36	19	
Female	16	6	
pT			0.06[a]
T1 + T2	49	19	
T3 + T4	3	6	
Pathological differentiation			0.51
Well	26	9	
Moderate	21	13	
Poor	5	3	
YK classification			0.43
YK1 + YK2 + YK3	34	14	
YK4C + YK4D	18	11	
Lymphovascular invasion			0.01
Negative	31	7	
Positive	21	18	
Perineural invasion			0.21
Negative	47	20	
Positive	5	5	
Sam68 expression			<0.01
High	33	6	
Low	19	19	

Pearson's chi-square test. [a]Fisher's exact test. P<0.05 was considered statistically significant in all analyses. CLNM, cervical lymph node metastasis; YK, Yamamoto-Kohama.

Table III. Multivariate analysis of the correlation between clinicopathological features and lymph node metastasis.

Clinicopathological features	Odds ratio	95%CI	P-value
Lymphovascular invasion (positive vs. negative)	2.75	0.93-8.59	0.07
Sam68 expression (high vs. low)	4.39	1.49-14.23	<0.01

Multivariate logistic regression analysis. P<0.05 was considered statistically significant. CLNM, cervical lymph node metastases; CI, confidence interval.

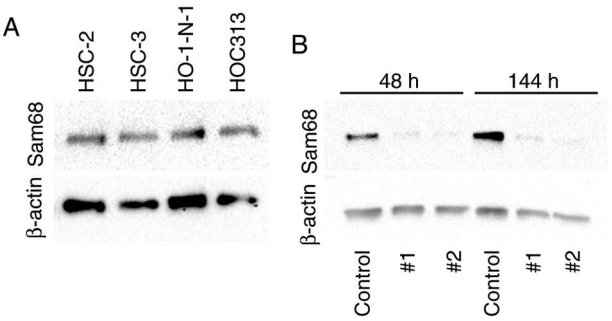

Figure 3. Expression of Sam68 in oral cancer cell lines. (A) Western blot analysis of Sam68 in oral cancer cells (HSC2, HSC3, HO-1-N-1, and HOC313). (B) Sam68 siRNA (#1 or #2) or control siRNA (control) was transfected into HO-1-N-1 cells, and the proteins were estimated at 48 or 144 h by western blotting. Sam68, Src-associated in mitosis 68 kDa.

sequencing was used to assess changes in the transcriptome between Sam68 siRNA- or control siRNA-transfected HO-1-N-1 cells. Differential expression analysis was performed and it was determined that genes with a false discovery rate of a P-value of <0.05 and a cutoff of |fold change|>2 were differentially expressed between the two conditions. A total of 150 differentially expressed genes (DEGs) were obtained including 20 upregulated and 130 downregulated genes (Fig. 4A). To explore the biological process significantly associated with these DEGs, GO enrichment analysis was further conducted. The results revealed that enriched GO terms were not detected in the upregulated genes; in addition, the downregulated genes were significantly concentrated in various biological processes (Fig. 4B). In the top 10 enriched processes, there were some processes related to the epithelial-mesenchymal transition (EMT): regulation of cell adhesion, epithelial cell differentiation, and mesenchyme development. Accumulating evidence has demonstrated that EMT, the transdifferentiation of epithelial cells into mesenchymal cells, is integral in cancer progression (36). Namely, epithelial cells downregulate their epithelial properties, lose their cell-cell adhesion, and acquire mesenchymal properties, which increase cell motility (36,37). Wound healing and chamber migration assays were used to confirm the effect of Sam68 on cell motility. As revealed in Fig. 4C, Sam68-knockdown cells demonstrated significantly slower wound closure compared with control cells. In addition, Sam68 knockdown markedly decreased the number of migrated cells as determined by the chamber migration assay (Fig. 4D). These data indicated that Sam68 may be associated with the EMT process and regulate the motility of OSCC cells.

To provide further validation, a literature search on the 36 downregulated DEGs enriched in the above 3 biological processes was conducted and a candidate gene associated with EMT and cell motility was selected. Vimentin is a classical mesenchymal marker that has been revealed to be elevated in EMT progression and related to motile activities (38). The differential expression of vimentin and other EMT markers were verified by RT-qPCR. As revealed in Fig. 5, a decreased mRNA level of vimentin was confirmed by qPCR in Sam68-knockdown cells. The mRNA level of epithelial (E-cadherin, cytokeratin 18, and plakophilin) and mesenchymal markers (N-cadherin and fibronectin) were not significantly altered by the reduction of Sam68 (Fig. 5). These

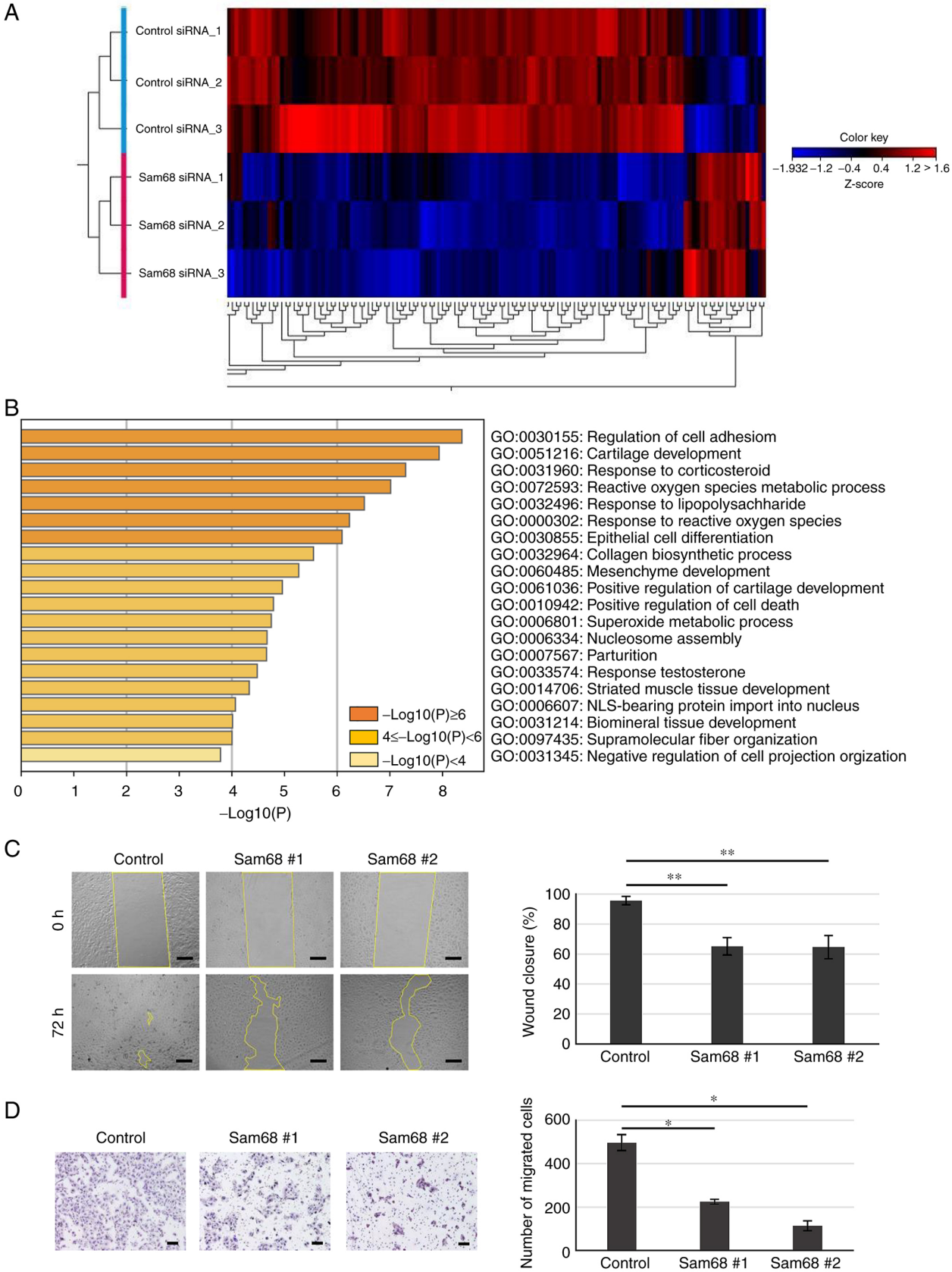

Figure 4. Inhibition of migration activity in Sam68-knockdown OSCC cells. (A) Heat map representation of 150 DEGs identified in mRNA sequencing between Sam68 siRNA #1-transfected HO-1-N-1 cells (n=3) and control siRNA-transfected cells (n=3). (B) GO enrichment analysis of 130 downregulated DEGs in Sam68-knockdown HO-1-N-1 cells. Bar graph of enriched GO terms (biological process) across input gene lists, colored by P-values. (C) HO-1-N-1 cells transfected with control siRNA (control) or Sam68 siRNA (Sam68 #1 or #2) were analyzed for wound closure at 72 h after wounding. Scale bar, 200 μm. Data are expressed as the mean ± SD. Dunnett's test compared with the control. **P<0.05. (D) HO-1-N-1 cells transfected with control siRNA (control) or Sam68 siRNA (Sam68 #1 or #2) were cultured in a Transwell chamber for 48 h. Migrated cells were stained and counted. Scale bar, 200 μm. Data are expressed as the mean ± SD. Dunnett's test compared with the control. *P<0.01. Sam68, Src-associated in mitosis 68 kDa; OSCC, oral squamous cell carcinoma; DEGs, differentially expressed genes; GO, Gene Ontology; siRNA, small interfering RNA.

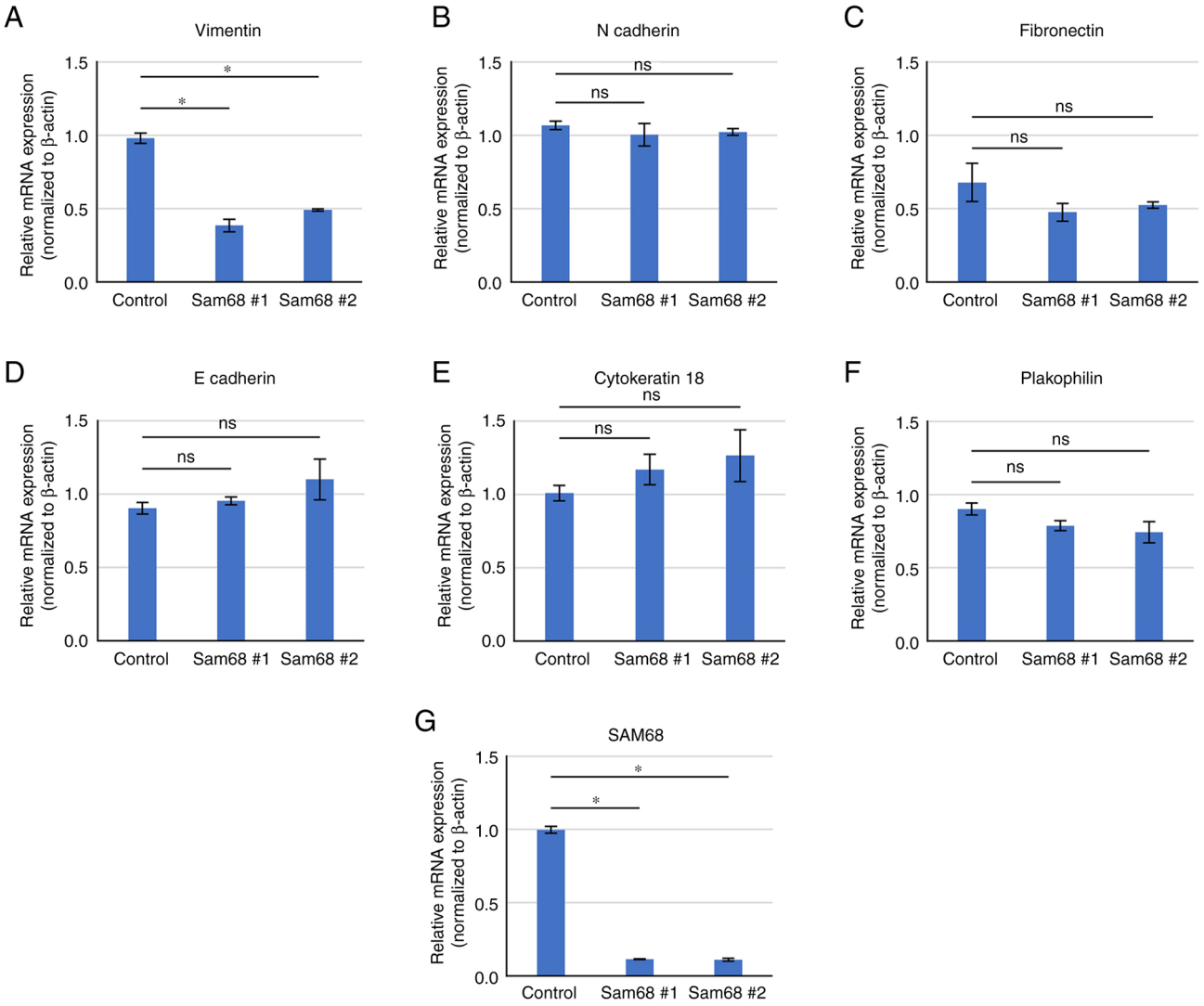

Figure 5. Validation of gene expression by RT-qPCR. (A and G) Comparison of mRNA expression of DEGs and (B-F) non-DEGs associated with the epithelial-mesenchymal transition between HO-1-N-1 cells transfected with control siRNA (control) or Sam68 siRNA (Sam68 #1 or #2). All data are expressed as the mean ± SD. Dunnett's test compared with the control. *P<0.01. ns, not significant. RT-qPCR, reverse transcription-quantitative PCR; DEGs, differentially expressed genes; siRNA, small interfering RNA; Sam68, Src-associated in mitosis 68 kDa; ns, not significant.

data were consistent with the results of mRNA sequencing, demonstrating that vimentin expression was specifically downregulated in Sam68-knockdown HO-1N-1 cells. The effect of Sam68 knockdown on vimentin expression was also assessed using RT-qPCR in other OSCC cell lines, and the mRNA expression of vimentin was confirmed to have been reduced via Sam68 knockdown in HSC-2 and HOC313 cells (Fig. S1). Collectively, these results indicated that Sam68 regulated vimentin expression and the motile mesenchymal phenotype of OSCC cells.

Association between Sam68 and vimentin expression on tissue samples of OSCC. Next, to clarify whether the expression of vimentin is correlated with that of Sam68 and cervical lymph node metastasis in OSCC, an immunohistochemical study of vimentin on 77 tissue samples was performed. Accordingly, 21 (27%) tumors were found to exhibit positive vimentin expression (Fig. 6). Although no statistical significance was observed, the proportion of tumors with Sam68 high expression was higher in the tumors exhibiting positive

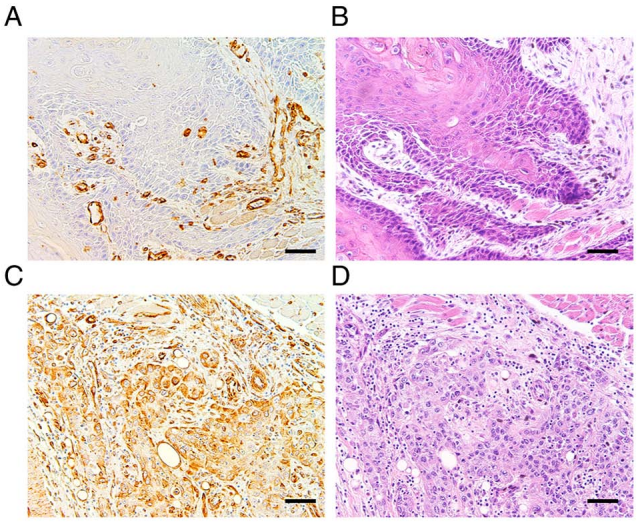

Figure 6. Immunohistochemical staining showing (A) negative and (C) positive expression of vimentin and (B and D) hematoxylin and eosin staining (magnification, x100; scale bar, 50 μm).

Table IV. Univariate analysis of the correlation between vimentin expression and Sam68 expression or cervical lymph node metastasis.

	Variables			
	Sam68 expression		Pathological CLNM	
	Low (n=39)	High (n=38)	Negative (n=52)	Positive (n=25)
Vimentin expression				
Negative	31	25	44	12
Positive	8	13	8	13
P-value	0.177		<0.01	

Pearson's chi-square test. P<0.05 was considered statistically significant. CLNM, cervical lymph node metastases.

vimentin expression (62%) than those tumors exhibiting negative vimentin expression (38%) (P=0.17; Table IV). A similar finding was confirmed in pT1 + T2 tumors (56 and 44%; P=0.26) or pT3 + 4 tumors (80 and 20%; P=0.34), respectively (data not shown). In addition, the univariate analysis showed that a positive expression of vimentin was significantly correlated with pathological cervical lymph node metastasis (P<0.01; Table IV).

Vimentin expression was reported to be upregulated at the invasive front in OSCC, which may be related to EMT (39). Thus, to obtain more insights into the association between expression of vimentin and Sam68, the distribution of positive vimentin and the pattern of Sam68 expression in the tumors exhibiting positive vimentin expression were investigated microscopically (n=21). Of the 21 tumors, six (28%) broadly exhibited positive vimentin expression at the invasive front, the central area, and the superficial area of the tumor. Similarly, the immunoreactivity of Sam68 was uniformly observed at almost all areas in these tumors. In 10/21 (48%) tumors, a positive vimentin expression was mostly observed at the deep area (the invasive front and the central area of the tumor) but not at the superficial areas of the tumors. Notably, in these tumors, the tumor cells with vimentin expression at the deep area were also observed to be accompanied with higher Sam68 immunoreactivity than those without vimentin expression at the superficial areas of the tumor (Fig. 7). In 3/21 (14%) tumors, positive vimentin expression was mostly observed at the deep area, but the immunoreactivity of Sam68 was uniformly observed at all areas in these tumors. In addition, in 2/21 (10%) tumors, the distribution of positive vimentin was broad, but Sam68 immunoreactivity was found to be higher at the deep area than those at the superficial area. These microscopic findings suggest that in the most tumors (16/21; 76%), the distribution of positive vimentin may be related to the distribution or degree of Sam68 expression. Collectively, these results support the association between vimentin expression and Sam68 expression as well as cervical lymph node metastasis in OSCC.

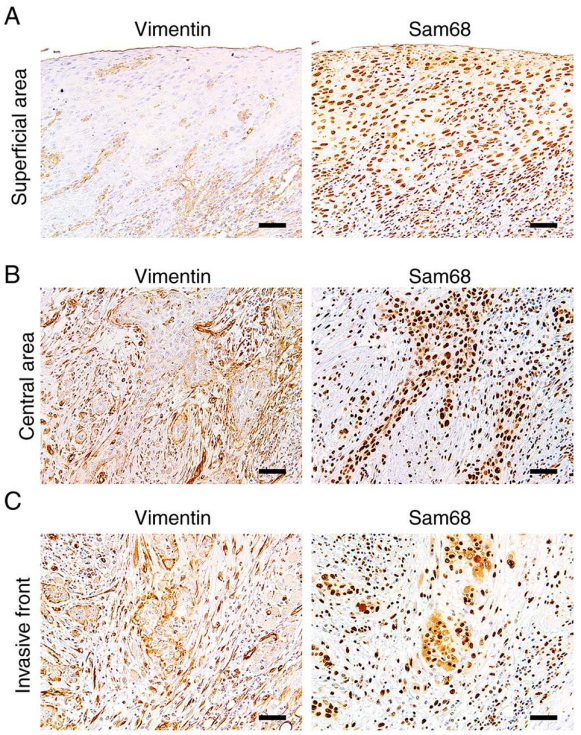

Figure 7. Immunohistochemistry of vimentin and Sam68 in the same tumor. (A) Representative image of the broad sheet of tumor cells without vimentin expression at the superficial area. (B) Representative image of the small cords of tumor cells exhibiting positive vimentin expression and higher Sam68 immunoreactivity at the central area. (C) Representative image of the small cords and clusters of tumor cells exhibiting positive vimentin expression and higher Sam68 immunoreactivity at the invasive front. (magnification, x100; scale bar, 50 μm). Sam68, Src-associated in mitosis 68 kDa.

Discussion

In the present study, the clinical implication of Sam68 in OSCC was demonstrated. The immunohistochemical results demonstrated that advanced OSCC exhibited significantly higher expression of Sam68. In particular, multivariate analysis demonstrated that a high expression of Sam68 was an independent factor associated with cervical lymph node metastasis in OSCC. Next, to elucidate the biological role of Sam68 in OSCC cells, mRNA sequencing was performed to measure the changes in the transcriptome via Sam68 knockdown. The GO analysis revealed that downregulated DEGs were enriched in the biological process related to EMT in Sam68-knockdown OSCC cells. It was established that vimentin expression was specifically downregulated in these cells. It was also confirmed that the migration activity of OSCC cells was significantly reduced by Sam68 knockdown. Furthermore, the immunohistochemical analyses of vimentin demonstrated the association between vimentin expression and Sam68 expression as well as

cervical lymph node metastasis. These results indicated that Sam68 may contribute to metastasis by regulating the expression of vimentin and the cell motility in OSCC.

Multiple studies have shown that Sam68 is associated with tumor progression, metastasis, and survival of patients in various cancers, including breast, prostate, lung, gastric, renal, and cervical cancers (9,18,21-26). However, few studies have investigated whether Sam68 has clinical and biological significance in OSCC. Chen *et al* conducted a univariate analysis and reported a correlation between higher Sam68 expression and T stage, N stage, nodal status, recurrence, and survival of patients with tongue cancer; however, these data were limited in patients with T1-3 classification and clinically negative nodal diseases (20). To the best of our knowledge, the present study is the first to assess the expression profile and evaluate the clinical implication of Sam68 in patients at all stages of OSCC. In this study, univariate analysis indicated that pathological T stage, lymphovascular invasion, and cervical lymph node metastasis were correlated with a high expression of Sam68 in OSCC. Moreover, multivariate analysis revealed that a high expression of Sam68 was an independent predictor of cervical lymph node metastasis. These results suggest that a high expression of Sam68 is closely related to tumor progression and metastasis to cervical lymph nodes in OSCC.

To evaluate the association between the invasive aspect of OSCC on histopathology and Sam68 expression, the histological grading was assessed by differentiation (2) and mode of invasion according to YK classification (27). In the results, those histological parameters were not significantly related to cervical lymph node metastasis. In addition, there were no statistically significant differences in those histological parameters between two groups of Sam68 expression. Conventional histological grading by differentiation was reported to have a limited predictive value for metastasis and prognosis (2,40,41), which is consistent with the result of the present study. In addition, other histological parameters based on the invasive pattern of tumors have been recognized to be associated with cervical lymph node metastasis (27,40). Conversely, similar to the result of the present study, some studies have shown no significant association between invasive pattern and metastasis in OSCC (41,42). A firm conclusion concerning the association between those histologic parameters and Sam68 expression cannot be obtained in the present study alone. Further studies are necessary to clarify the association between them.

A previous study revealed the association between Sam68 and resistance to anticancer agents in tongue SCC cells (20); however, there are no data in the literature regarding the malignant phenotypes affected by dysregulation of Sam68 in OSCC. To obtain new insights into the biological significance of Sam68 in OSCC, mRNA sequencing was performed to investigate changes in the gene expression profile through Sam68 knockdown. This result revealed that 36 downregulated DEGs were statistically enriched in the biological process of GO related to EMT, including regulation of cell adhesion, epithelial cell differentiation, and mesenchyme development (36,37,43). EMT plays a critical role in tumor progression and metastasis (36-38,44). During this process, epithelial cells lose cell-cell adhesion and apicobasal polarity to exhibit migratory mesenchymal properties (36). It was verified that Sam68 knockdown significantly reduced motile behavior and vimentin expression in OSCC cells. The immunohistochemical analysis of vimentin also indicated the association between positive vimentin and Sam68 expression. In addition, a positive vimentin expression was found to be significantly correlated with cervical lymph node metastasis in this study. Recent lines of evidence have demonstrated that vimentin expression is upregulated in EMT progression, resulting in a more motile phenotype of tumor cells (37,38). During the progression of EMT, epithelial markers such as keratin, E-cadherin, and plakophilin are decreased and mesenchymal markers such as vimentin, N-cadherin, and fibronectin are increased (36). However, the expression profile of EMT markers has been reported to be widely varied depending on the cancer type, cell lines, and signaling pathways of EMT (45-47). Saito *et al* demonstrated that various OSCC cell lines exhibited each specific expression of EMT markers (46). In addition, the cell status in which epithelial properties are retained, known as partial EMT, has been recognized to possess a higher metastatic ability as compared with complete EMT, with loss of all epithelial features and complete acquisition of mesenchymal morphology (48-50). In this study, vimentin was specifically regulated by Sam68 in OSCC cells; by contrast, other epithelial and mesenchymal markers were not significantly altered in these cells. Taken together, the results indicated that Sam68 may regulate the expression of vimentin to induce partial EMT and promote the motile mesenchymal behavior of OSCC.

It has been recognized that changes at the RNA level, including alternative splicing and noncoding RNA-mediated control, regulate EMT (19,36). As a result of alternative splicing, extensive isoforms are generated in various proteins that regulate EMT. Valacca *et al* demonstrated that Sam68 contributes to the regulation of EMT by changing the splicing profile and overall transcription levels of serine/arginine-rich splicing factor 1 (SRSF1), which produces a constitutively active splicing variant of Recepteur d'Origine Nantais (Ron) proto-oncogene in colon adenocarcinoma cells (19). In the present study, an analysis of alternative splicing variants using RNA-sequencing data was also performed. The results did not reveal a significant difference in SRSF1 or Ron splicing variants between Sam68-knockdown OSCC cells and control cells (data not shown). In addition, recent research has demonstrated that *O*-GlcNAcylation of Sam68 may enhance the migratory and invasive abilities of lung cancer cells (51). *O*-GlcNAcylation is a post-translational protein modification catalyzed by *O*-GlcNAc transferase (OGT) and has been linked to biological properties of cancer, including cell proliferation, survival, invasion, and metastasis (51,52). It has also been reported that the EMT process is associated with modulation of *O*-GlcNAcylation in lung cancer cells (52). In the present study, the RNA-sequencing data showed that the mRNA level of OGT was not significantly altered via Sam68-knockdown in OSCC (data not shown). Collectively, these findings suggest that Sam68 may have the potential to promote EMT in a different manner, depending on the type of cancer.

The present study has some limitations. First, is the relatively small number of patients included in the study. Second, the sample size between the two groups of pT stage, perineural invasion, and primary recurrence were biased. Therefore, the statistical power to draw firm conclusions was insufficient.

Collectively, the findings of the present study indicated that Sam68 contributes to metastasis by regulating the expression of vimentin, which may be associated with partial EMT and the cell motility of OSCC. Although the detailed pathways by which Sam68 induces vimentin remain to be identified, it is concluded that Sam68 may be a promising predictor of cervical lymph node metastasis and have the potential to be a novel therapeutic target in oral cancer.

Acknowledgements

The authors would like to thank Professor Jun Aida (Department of Oral Health Promotion, Graduate School of Medical and Dental Sciences, Tokyo Medical and Dental University, Tokyo, Japan) for his valuable advice on statistical analysis. We are grateful to Associate Professor Kei-ichi Morita (Department of Maxillofacial Surgery, Graduate School of Medical and Dental Sciences, Tokyo Medical and Dental University, Tokyo, Japan) for his technical support.

Funding

The present study was supported by JSPS KAKENHI (grant no. 20K10133).

Availability of data and materials

The data sets used and/or analyzed during the present study are available from the corresponding author upon reasonable request. The RNA sequencing data as FASTQ files and expression browser as table data are deposited in the Gene Expression Omnibus (https://www.ncbi.nlm.nih.gov/geo/) under accession number: GSE202136.

Authors' contributions

TKu conceived the present study. TKu and FH designed the experiments. TKo, YI, HHi, FT, YM, and KK collected the clinical and pathological data of patients. TKo, TS, and SF performed the experiments and analyzed these data. TKu and TKo analyzed statistical data. TKu and HHa confirm the authenticity of all the raw data. TKu and TKo wrote the manuscript. All authors read and approved the final version of the manuscript.

Ethics approval and consent to participate

The study complied with the standards of the Declaration of Helsinki and was approved (approval no. D2020-025) by the Institutional Review Board of Tokyo Medical and Dental University (Tokyo, Japan).

Patient consent for publication

Opt-out informed consent from patients was obtained by exhibiting the research information on the official website of our hospital (Tokyo Medical and Dental University Hospital, Tokyo, Japan). The authors guarantee the opportunity for refusal by document, call or e-mail whenever possible. Patients who rejected participation in this study were excluded.

Competing interests

The authors declare that they have no competing interests.

References

1. Bray F, Ferlay J, Soerjomataram I, Siegel RL, Torre LA and Jemal A: Global cancer statistics 2018: GLOBOCAN estimates of incidence and mortality worldwide for 36 cancers in 185 countries. CA Cancer J Clin 68: 394-424, 2018.
2. El-Naggar AK, Chan JKC, Grandis JR, Takata T and Slootweg PJ: WHO classification of head and neck tumours. 4th edition. IARC Press, Lyon, 2017.
3. Sato J, Kitagawa Y, Watanabe S, Asaka T, Ohga N, Hirata K, Shiga T, Satoh A and Tamaki N: Hypoxic volume evaluated by ^{18}F-fluoromisonidazole positron emission tomography (FMISO-PET) may be a prognostic factor in patients with oral squamous cell carcinoma: Preliminary analyses. Int J Oral Maxillofac Surg 47: 553-560, 2018.
4. Larsen SR, Johansen J, Sørensen JA and Krogdahl A: The prognostic significance of histological features in oral squamous cell carcinoma. J Oral Pathol Med 38: 657-662, 2009.
5. Oikawa Y, Kugimoto T, Kashima Y, Okuyama K, Ohsako T, Kuroshima T, Hirai H, Tomioka H, Shimamoto H, Michi Y and Harada H: Surgical treatment for oral tongue squamous cell carcinoma: A retrospective study of 432 patients. Glob Health Med 3: 157-162, 2021.
6. Tomioka H, Yamagata Y, Oikawa Y, Ohsako T, Kugimoto T, Kuroshima T, Hirai H, Shimamoto H and Harada H: Risk factors for distant metastasis in locoregionally controlled oral squamous cell carcinoma: A retrospective study. Sci Rep 11: 5213, 2021.
7. Kuroshima T, Onozato Y, Oikawa Y, Ohsako T, Kugimoto T, Hirai H, Tomioka H, Michi Y, Miura M, Yoshimura R and Harada H: Prognostic impact of lingual lymph node metastasis in patients with squamous cell carcinoma of the tongue: A retrospective study. Sci Rep 11: 20535, 2021.
8. Vernet C and Artzt K: STAR, a gene family involved in signal transduction and activation of RNA. Trends Genet 13: 479-484, 1997.
9. Bielli P, Busà R, Paronetto MP and Sette C: The RNA-binding protein Sam68 is a multifunctional player in human cancer. Endocr Relat Cancer 18: R91-R102, 2011.
10. Henao-Mejia J and He JJ: Sam68 relocalization into stress granules in response to oxidative stress through complexing with TIA-1. Exp Cell Res 315: 3381-3395, 2009.
11. Wu J, Zhou L, Tonissen K, Tee R and Artzt K: The quaking I-5 protein (QKI-5) has a novel nuclear localization signal and shuttles between the nucleus and the cytoplasm. J Biol Chem 274: 29202-29210, 1999.
12. Li J, Liu Y, Kim BO and He JJ: Direct participation of Sam68, the 68-kilodalton Src-associated protein in mitosis, in the CRM1-mediated Rev nuclear export pathway. J Virol 76: 8374-8382, 2002.
13. Babic I, Cherry E and Fujita DJ: SUMO modification of Sam68 enhances its ability to repress cyclin D1 expression and inhibits its ability to induce apoptosis. Oncogene 25: 4955-4964, 2006.
14. Paronetto MP, Achsel T, Massiello A, Chalfant CE and Sette C: The RNA-binding protein Sam68 modulates the alternative splicing of Bcl-x. J Cell Biol 176: 929-939, 2007.
15. Hong W, Resnick RJ, Rakowski C, Shalloway D, Taylor SJ and Blobel GA: Physical and functional interaction between the transcriptional cofactor CBP and the KH domain protein Sam68. Mol Cancer Res 1: 48-55, 2002.
16. Richard S, Torabi N, Franco GV, Tremblay GA, Chen T, Vogel G, Morel M, Cléroux P, Forget-Richard A, Komarova S, *et al*: Ablation of the Sam68 RNA binding protein protects mice from age-related bone loss. PLoS Genet 1: e74, 2005.
17. Iijima T, Wu K, Witte H, Hanno-Iijima Y, Glatter T, Richard S and Scheiffele P: SAM68 regulates neuronal activity-dependent alternative splicing of neurexin-1. Cell 147: 1601-1614, 2011.
18. Frisone P, Pradella D, Di Matteo A, Belloni E, Ghigna C and Paronetto MP: SAM68: Signal transduction and RNA metabolism in human cancer. Biomed Res Int 2015: 528954, 2015.
19. Valacca C, Bonomi S, Buratti E, Pedrotti S, Baralle FE, Sette C, Ghigna C and Biamonti G: Sam68 regulates EMT through alternative splicing-activated nonsense-mediated mRNA decay of the SF2/ASF proto-oncogene. J Cell Biol 191: 87-99, 2010.

20. Chen S, Li H, Zhuang S, Zhang J, Gao F, Wang X, Chen W and Song M: Sam68 reduces cisplatin-induced apoptosis in tongue carcinoma. J Exp Clin Cancer Res 35: 123, 2016.
21. Xiao J, Wang Q, Yang Q, Wang H, Qiang F, He S, Cai J, Yang L and Wang Y: Clinical significance and effect of Sam68 expression in gastric cancer. Oncol Lett 15: 4745-4752, 2018.
22. Li X, Zhou X, Hua F, Fan Y, Zu L, Wang Y, Shen W, Pan H and Zhou Q: The RNA-binding protein Sam68 is critical for non-small cell lung cancer cell proliferation by regulating Wnt/β-catenin pathway. Int J Clin Exp Pathol 10: 8281-8291, 2017.
23. Li Z, Yu CP, Zhong Y, Liu TJ, Huang QD, Zhao XH, Huang H, Tu H, Jiang S, Zhang Y, *et al*: Sam68 expression and cytoplasmic localization is correlated with lymph node metastasis as well as prognosis in patients with early-stage cervical cancer. Ann Oncol 23: 638-646, 2012.
24. Zhang Z, Li J, Zheng H, Yu C, Chen J, Liu Z, Li M, Zeng M, Zhou F and Song L: Expression and cytoplasmic localization of SAM68 is a significant and independent prognostic marker for renal cell carcinoma. Cancer Epidemiol Biomarkers Prev 18: 2685-2693, 2009.
25. Sumithra B, Saxena U and Das AB: A comprehensive study on genome-wide coexpression network of KHDRBS1/Sam68 reveals its cancer and patient-specific association. Sci Rep 9: 11083, 2019.
26. Song L, Wang L, Li Y, Xiong H, Wu J, Li J and Li M: Sam68 up-regulation correlates with, and its down-regulation inhibits, proliferation and tumourigenicity of breast cancer cells. J Pathol 222: 227-237, 2010.
27. Yamamoto E, Kohama G, Sunakawa H, Iwai M and Hiratsuka H: Mode of invasion, bleomycin sensitivity, and clinical course in squamous cell carcinoma of the oral cavity. Cancer 51: 2175-2180, 1983.
28. Edge SB, Byrd DR, Compton CC, Fritz AG, Greene FL and Trotti AA (eds): American Joint Committee on Cancer: AJCC cancer staging manual. 7th edition. Springer-Verlag, New York, 2009.
29. Costa LC, Leite CF, Cardoso SV, Loyola AM, Faria PR, Souza PE and Horta MC: Expression of epithelial-mesenchymal transition markers at the invasive front of oral squamous cell carcinoma. J Appl Oral Sci 23: 169-178, 2015.
30. Tran CM, Kuroshima T, Oikawa Y, Michi Y, Kayamori K and Harada H: Clinicopathological and immunohistochemical characteristics of pigmented oral squamous cell carcinoma. Oncol Lett 21: 339, 2021.
31. Momose F, Araida T, Negishi A, Ichijo H, Shioda S and Sasaki S: Variant sublines with different metastatic potentials selected in nude mice from human oral squamous cell carcinomas. J Oral Pathol Med 18: 391-395, 1989.
32. Tadokoro K, Ueda M, Ohshima T, Fujita K, Rikimaru K, Takahashi N, Enomoto S and Tsuchida N: Activation of oncogenes in human oral cancer cells: A novel codon 13 mutation of c-H-ras-1 and concurrent amplifications of c-erbB-1 and c-myc. Oncogene 4: 499-505, 1989.
33. Livak KJ and Schmittgen TD: Analysis of relative gene expression data using real-time quantitative PCR and the 2(-Delta Delta C(T)) method. Methods 25: 402-408, 2001.
34. Tamai S, Fujita SI, Komine R, Kanki Y, Aoki K, Watanabe K, Takekoshi K and Sugasawa T: Acute cold stress induces transient MuRF1 upregulation in the skeletal muscle of zebrafish. Biochem Biophys Res Commun 608: 59-65, 2022.
35. Zhou Y, Zhou B, Pache L, Chang M, Khodabakhshi AH, Tanaseichuk O, Benner C and Chanda SK: Metascape provides a biologist-oriented resource for the analysis of systems-level datasets. Nat Commun 10: 1523, 2019.
36. Lamouille S, Xu J and Derynck R: Molecular mechanisms of epithelial-mesenchymal transition. Nat Rev Mol Cell Biol 15: 178-196, 2014.
37. Le Bras GF, Taubenslag KJ and Andl CD: The regulation of cell-cell adhesion during epithelial-mesenchymal transition, motility and tumor progression. Cell Adh Migr 6: 365-373, 2012.
38. Sun BO, Fang Y, Li Z, Chen Z and Xiang J: Role of cellular cytoskeleton in epithelial-mesenchymal transition process during cancer progression. Biomed Rep 3: 603-610, 2015.
39. Kurihara K, Isobe T, Yamamoto G, Tanaka Y, Katakura A and Tachikawa T: Expression of BMI1 and ZEB1 in epithelial-mesenchymal transition of tongue squamous cell carcinoma. Oncol Rep 34: 771-778, 2015.
40. Xu B, Salama AM, Valero C, Yuan A, Khimraj A, Saliba M, Zanoni DK, Ganly I, Patel SG, Katabi N and Ghossein R: The prognostic role of histologic grade, worst pattern of invasion, and tumor budding in early oral tongue squamous cell carcinoma: A comparative study. Virchows Arch 479: 597-606, 2021.
41. Kane SV, Gupta M, Kakade AC and D' Cruz A: Depth of invasion is the most significant histological predictor of subclinical cervical lymph node metastasis in early squamous carcinomas of the oral cavity. Eur J Surg Oncol 32: 795-803, 2006.
42. Kolokythas A, Park S, Schlieve T, Pytynia K and Cox D: Squamous cell carcinoma of the oral tongue: Histopathological parameters associated with outcome. Int J Oral Maxillofac Surg 44: 1069-1074, 2015.
43. Guan Y, Xu F, Wang Y, Tian J, Wan Z, Wang Z and Chong T: Identification of key genes and functions of circulating tumor cells in multiple cancers through bioinformatic analysis. BMC Med Genomics 13: 140, 2020.
44. Han Y, Yamada SI, Kawamoto M, Gibo T, Hashidume M, Otagiri H, Tanaka H, Takizawa A, Kondo E, Sakai H, *et al*: Immunohistochemical investigation of biomarkers for predicting adipose tissue invasion in oral squamous cell carcinoma. J Oral Maxillofac Surg Med Pathol 34: 507-513, 2022.
45. Peinado H, Olmeda D and Cano A: Snail, Zeb and bHLH factors in tumour progression: An alliance against the epithelial phenotype? Nat Rev Cancer 7: 415-428, 2007.
46. Saito D, Kyakumoto S, Chosa N, Ibi M, Takahashi N, Okubo N, Sawada S, Ishisaki A and Kamo M: Transforming growth factor-β1 induces epithelial-mesenchymal transition and integrin α3β1-mediated cell migration of HSC-4 human squamous cell carcinoma cells through Slug. J Biochem 153: 303-315, 2013.
47. Zeisberg M and Neilson EG: Biomarkers for epithelial-mesenchymal transitions. J Clin Invest 119: 1429-1437, 2009.
48. Jolly MK, Somarelli JA, Sheth M, Biddle A, Tripathi SC, Armstrong AJ, Hanash SM, Bapat SA, Rangarajan A and Levine H: Hybrid epithelial/mesenchymal phenotypes promote metastasis and therapy resistance across carcinomas. Pharmacol Ther 194: 161-184, 2019.
49. Saitoh M: Involvement of partial EMT in cancer progression. J Biochem 164: 257-264, 2018.
50. Sakakitani S, Podyma-Inoue KA, Takayama R, Takahashi K, Ishigami-Yuasa M, Kagechika H, Harada H and Watabe T: Activation of β2-adrenergic receptor signals suppresses mesenchymal phenotypes of oral squamous cell carcinoma cells. Cancer Sci 112: 155-167, 2021.
51. Lin CH, Liao CC, Wang SY, Peng CY, Yeh YC, Chen MY and Chou TY: Comparative O-GlcNAc proteomic analysis reveals a role of O-GlcNAcylated SAM68 in lung cancer aggressiveness. Cancers (Basel) 14: 243, 2022.
52. Lucena MC, Carvalho-Cruz P, Donadio JL, Oliveira IA, de Queiroz RM, Marinho-Carvalho MM, Sola-Penna M, de Paula IF, Gondim KC, McComb ME, *et al*: Epithelial mesenchymal transition induces aberrant glycosylation through hexosamine biosynthetic pathway activation. J Biol Chem 291: 12917-12929, 2016.